Numerical study of the shape and integral parameters of a dendrite

R. González-Cinca* and L. Ramírez-Piscina
Departament de Física Aplicada, Universitat Politècnica de Catalunya, Avinguda del Canal Olímpic s/n, 08860 Castelldefels, Barcelona, Spain
(Received 16 June 2004; published 30 November 2004)

We present a numerical study of sidebranching of a solidifying dendrite by means of a phase-field model. Special attention is paid to the regions far from the tip of the dendrite, where linear theories are no longer valid. Two regions have been distinguished outside the linear region: a first one in which sidebranching is in a competition process and a second one further down where branches behave as independent of each other. The shape of the dendrite and integral parameters characterizing the whole dendrite (contour length and area of the dendrite) have been computed and related to the characteristic tip radius for both surface tension and kinetic dominated dendrites. Conclusions about the different behaviors observed and comparison with available experiments and theoretical predictions are presented.

DOI: 10.1103/PhysRevE.70.051612 PACS number(s): 81.10.Aj, 81.10.Dn, 64.70.Dv

I. INTRODUCTION

The generation of dendritic patterns arises in different nonequilibrium situations [1–8]. The case of dendrites appearing during the solidification of a melt has long provided an archetypical example of a pattern forming system, in which the underlying physics is well known. Nonetheless, from the theoretical point of view it has posed a number of nontrivial questions on the selection of the final growth mode, which in a large amount has driven the research on the effects of nonlinearities, anisotropies, and fluctuations in interfacial pattern formation. These questions also have an applied interest, since solidification is one of the most common methods to produce materials. It is well known that the details of the dendritic pattern (and in particular its associated scales) appearing during growth determine the microstructure of the grown solid, which in turn is responsible to a large degree for its final (mechanical and electrical) properties [9].

In this context increasing attention is focused on the shape of the growing dendrite and on sidebranching [10–37], which corresponds to the appearance and growth of secondary branches at both sides of the dendrite. Sidebranching activity shows different behaviors depending on the distance to the tip of the dendrite [16,34,35]. In the zone closer to the tip sidebranches are created as a convective instability of the dendrite and grow linearly. Further down from the tip, sidebranches are usually much more developed and a competition process between branches takes place mediated by the interaction between their diffused fields. Much further from the tip, the competition has finished and the winner branches grow as free dendrites while the growth of looser branches is inhibited.

Many theoretical [12–20] and experimental [21–35] studies of the region close to the tip have been carried out in recent years. A common point in the study of the linear region has been the characterization of sidebranching by means of its amplitude and wavelength. The growth of sidebranches in the regions further down from the tip presents a behavior very different from that of the linear regime. One finds first a region where branches compete, interacting through the expelled heat. This gives rise to an irregular growth of sidebranches which is difficult to characterize by their amplitude and wavelength, since these quantities are no longer well defined outside the linear region. Experiments carried out with different substances [25,26,30] have shown that sidebranching in this region is self-similar and that geometrical parameters can be scaled by the tip radius R. This nonlinear region and its associated self-similar growth have their limits at distances to the tip of the order of the diffusion length, i.e., $z/R \ll 1/\mathrm{Pe}$ [16], where Pe is the Péclet number. Further down, sidebranches behave like dendrites themselves.

The nonlinear region has been intensively studied in experiments with xenon dendrites by Hürlimann *et al.* [26] and with succinonitrile dendrites by Li and Beckermann [30,31]. In particular, the shape of the sidebranching envelope was studied in Ref. [30] by measuring the distance X from the axis of the dendrite to the tip of active sidebranches (defined as those branches longer than all the other branches closer to the tip) versus the distance Z to the tip along the axis of the dendrite (see Fig. 1). Values of X and Z were computed from the image of the dendrite projected on a plane, and far from the tip the relation $X/R = 0.668(Z/R)^{0.859}$ was obtained.

An alternative set of integral parameters was proposed in Refs. [26,30] in order to describe the complex shape of a dendrite as a whole and the nonlinearities of dendritic solidification. Parameters characterizing independent parts of the dendrite (e.g., amplitude and wavelength of the sidebranching) do not take into account the interaction of the sidebranches through the diffusion field. Nonlinear effects such as, e.g., coarsening, make unclear which sidebranches should be included in the measurement of the wavelength and which others should not. Instead, the contour length U, the projection area F, and the volume of a dendrite appear to be more appropriate.

It was found in the earlier experimental work of Refs. [26,30] that the projection area varied linearly with the con-

*FAX: (34) 934137007; email address: ricard@fa.upc.es

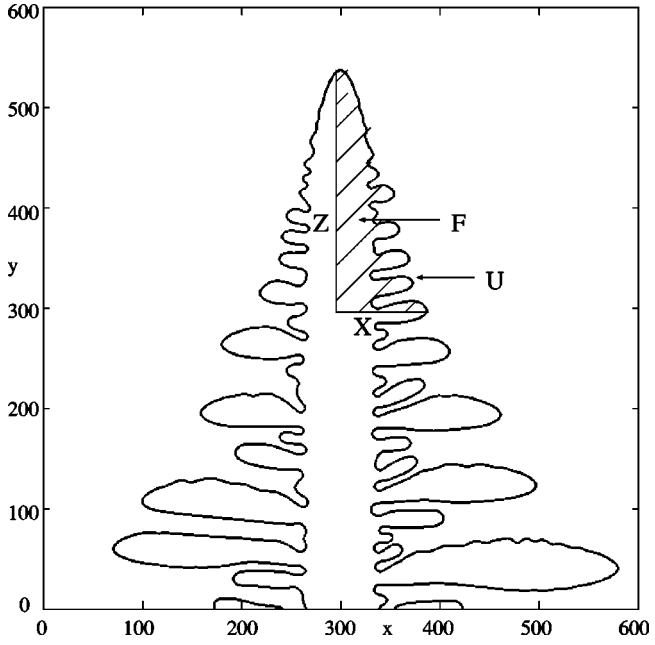

FIG. 1. Example of dendrite obtained at $\Delta=0.575$. Distances Z and X of active sidebranches used to characterize the shape of the dendrite, and the integral parameters contour length (U) and surface area (F), are indicated.

tour length and the corresponding slope M satisfied $M/R=\text{const}$. Similar results were found in early simulations [36], but this was shown to be an effect of reflecting boundary conditions strongly affecting the dendrite [37]. This suggests that the experimental observations could have been affected by the diffusion field of other close dendrites or other growing morphologies. In more recent experimental [31] and numerical [37] work it was obtained that $F/(UR)$ was not a constant in the nonlinear regime.

The projection area showed two different behaviors [$F/R^2=0.847(Z/R)^{1.598}$ for $Z/R<30$ and $F/R^2=0.578(Z/R)^{1.72}$ for $Z/R>30$] in three-dimensional succinonitrile dendrites [31]. However, in two-dimensional ammonium bromide dendrites [22], the area F was found to vary over three orders of magnitude as $Z^{1.5}$, as would have happened if the dendrites had had a smooth parabolic shape. As regards the variation of the contour length with the distance to the tip, only data corresponding to three-dimensional dendrites are available, where two behaviors are distinguished [$U/R=0.887(Z/R)^{1.116}$ for $Z/R<20$ and $U/R=0.378(Z/R)^{1.50}$ for $Z/R>40$] [31].

An additional question is whether strong undercooling can produce qualitative changes in sidebranching characteristics. It is well known that on increasing undercooling the growth can switch from a regime dominated by surface tension to a regime dominated by kinetic effects. This was already predicted theoretically in Ref. [4]. When anisotropies of both effects favor different directions, changes in the growth directions of both dendrite and branches occur on changing the undercooling. Even if these anisotropies are in the same direction, the behavior of the tip radius and velocity can present abrupt changes. Numerical evidence of such changes can be found in Ref. [45].

In this paper we present a study of sidebranching by means of a phase-field model for moving solid-liquid interfaces [38–44]. We consider sidebranching generated by selective amplification of fluctuations near the tip of a free growing dendrite. In particular, we focus on the nonlinear zone, including both the region where competition occurs and further down where sidebranches behave as free growing dendrites. Characterization is performed by working out the shape of the dendrite by means of its envelope, and calculating the integral parameters. We have varied undercooling in a large range, in particular reaching relatively high values of the undercooling. This has permitted us, on the one hand, due to reduction in diffusion length, to access the region of free growing sidebranches far from the tip, and, on the other hand, to reach the kinetic regime of growth.

This paper is organized as follows. In Sec. II we present the classical sharp-interface model that characterizes a solidification system, the phase-field model, and the numerical procedure used in this work. In Sec. III we present the results of simulations. We particularize the effect of varying undercooling, and the differences between different zones of the dendrite. Detailed characterization of the whole dendrite is performed by its shape and by computing the integral parameters. Finally, concluding remarks are presented in Sec. IV.

II. MODEL AND NUMERICAL PROCEDURE

The free solidification of a pure substance can be described by the sharp-interface model [1], which relies on the heat diffusion equation together with two boundary conditions at the interface, namely, heat conservation and the Gibbs-Thomson (local equilibrium) equation:

$$\frac{\partial T}{\partial t}=D\nabla^2 T, \tag{2.1}$$

$$L v_n = Dc_p[(\nabla_n T)_S-(\nabla_n T)_L], \tag{2.2}$$

$$T_{\text{interface}}=T_M-\frac{T_M}{L}[\sigma(\theta)+\sigma''(\theta)]\kappa-v_n\beta_k(\theta). \tag{2.3}$$

In these equations T is the temperature (T_M being the melting one), D is the diffusion coefficient ($D=k/c_p$, k being the heat conductivity and c_p the specific heat per unit volume), L is the latent heat per unit volume, v_n is the normal velocity of the interface, ∇_n is the normal derivative at the interface (S and L referring to solid and liquid, respectively), $\sigma(\theta)$ is the anisotropic surface tension (where θ is the angle between the normal to the interface and some crystallographic axis), and κ is the local curvature of the interface. $\beta_k(\theta)$ is an anisotropic kinetic term, introduced into the Gibbs-Thomson equation (2.3) to account for a linear nonequilibrium correction.

The results of simulations presented below have been obtained by means of a phase-field model. These kinds of model have received increased attention during recent years [44]. One of their main features is the introduction of an additional nonconserved scalar order parameter or phase field ϕ, whose time evolution equation is coupled with the

heat diffusion equation through a source term in order to take into account the boundary conditions at the interface. The phase field takes constant values in each of the bulk phases (in our case, $\phi=0$ in the solid and $\phi=1$ in the liquid) changing continuously between them over a transition layer, the interfacial thickness ϵ. The equations of the model are then constructed in such a way that they converge to the sharp-interface dynamics of Eqs. (2.1), (2.2), and (2.3) in the limit of vanishing ϵ. Hence this parameter controls the convergence to the sharp-interface limit.

The corresponding equations for the time evolution of the phase field and the dimensionless temperature can be written in the following form [39]:

$$\epsilon^2\tau(\theta)\frac{\partial\phi}{\partial t} = \phi(1-\phi)\left(\phi-\frac{1}{2}+30\epsilon\beta\Delta u\phi(1-\phi)\right) - \epsilon^2\frac{\partial}{\partial x}\left[\eta(\theta)\eta'(\theta)\frac{\partial\phi}{\partial y}\right] + \epsilon^2\frac{\partial}{\partial y}\left[\eta(\theta)\eta'(\theta)\frac{\partial\phi}{\partial x}\right] + \epsilon^2\nabla[\eta^2(\theta)\nabla\phi], \tag{2.4}$$

$$\frac{\partial u}{\partial t}+\frac{1}{\Delta}(30\phi^2-60\phi^3+30\phi^4)\frac{\partial\phi}{\partial t} = \nabla^2 u+\psi(x,y,t), \tag{2.5}$$

where $u(\mathbf{r},t)$ is the diffusion field and $\Delta=c_p\Delta T/L$ is the dimensionless undercooling. Lengths are scaled by some arbitrary reference length ω, while times are scaled by ω^2/D. In these equations θ is the angle between the x axis and the gradient of the phase field. $\eta(\theta)=\sigma(\theta)/\sigma(0)$ is the anisotropy of the surface tension. $\tau(\theta)$ is given by $(c_pD/Ld_0)\eta(\theta)\beta_k(\theta)$, so the anisotropy of the kinetic term is given by $\tau(\theta)/\eta(\theta)$. β is equal to $\sqrt{2}\omega/12d_0$ and $d_0=c_pT_M\sigma(0)/L^2$ is the capillary length.

A source of fluctuations is introduced through the additive term ψ in the heat equation. It was demonstrated [20] that sidebranching induced by this kind of noise qualitatively reproduces the characteristics of the (thermodynamical) internal noise, which makes it appropriate for the study of sidebranching. In our two-dimensional simulations the noise term is evaluated at each cell (i,j) of lateral size Δx as Ir_{ij}, where I denotes the amplitude of the noise, and r_{ij} is an uncorrelated uniform random number in the interval $[-0.5,0.5]$. The phase-field model equations have been solved on rectangular lattices using first-order finite differences on a uniform grid with mesh spacing Δx. An explicit time-differencing scheme has been used to solve the equation for ϕ, whereas for the u equation the alternating-direction implicit method was chosen [46]. The kinetic term has been taken as isotropic, which leads to $\tau(\theta)=m\eta(\theta)$ with constant m. A fourfold surface tension anisotropy $\eta(\theta)=1+\gamma\cos(4\theta)$ has been considered.

The growth morphologies have been obtained by setting a small vertical seed $(\phi=0,u=0)$ in the center of the bottom side of the system and imposing $\phi=1$ and $u=-1$ on the rest of the system. Symmetric boundary conditions for ϕ and u have been used on the four sides of the system. Special care has been taken to employ large enough system sizes to avoid any influence of boundary conditions on the results presented throughout this paper.

We have used a set of phase-field model parameters that gives rise to a growing needle without sidebranching when no noise $(I=0)$ is added to the simulations. This assures us that the sidebranching observed when $I\neq 0$ is not due to numerical noise. The fixed parameters for all the simulations have been $\beta=320$, $\gamma=0.045$, $m=16$, and $\epsilon=3.75\times10^{-3}$. The value of Δ has been varied in the range 0.44–0.65. The noise amplitude was kept constant $(I=16)$ in all the simulations and the time and spatial discretizations used were $\Delta t=1.25\times10^{-4}$ and $\Delta x=0.0125$.

Under these conditions, the obtained morphologies were dendrites with three main arms growing from the seed, one in the vertical (y) direction and two in the horizontal (x) one. We have focused on the sidebranches which grew perpendicular to the vertical arm. Thus, in order to get rid of the influence of the diffusion field of the horizontal arms on these sidebranches, we have been forced to run long simulations and only observe an area at a fixed distance to the tip. In order to avoid working with unnecessarily large systems, we have performed periodic shifts of the complete system, a practice that has been checked to not affect the results of the simulation. In Fig. 1 we show an example of a typical grown dendrite.

III. RESULTS AND DISCUSSION

A first series of simulations was performed exploring the effect of undercooling on the tip radius. This was measured by computing $R=\phi_x/\phi_{yy}$ at the tip of the dendrites [39]. The aim was to identify different regimes of growth in a large range of Δ. In our case, anisotropy is only considered in surface tension. Thus, when the undercooling is changed no change in growth direction is expected although the behavior of the tip radius and velocity may vary. In particular in the surface tension controlled regime the tip radius should decrease (together with increase of tip velocity) by increasing undercooling. On the contrary in the kinetic regime, with an isotropic kinetic term, one expects larger tip radius at higher velocities. In Fig. 2 is shown the behavior of the tip radius as a function of the undercooling. A change of the behavior around the value 0.575 can be clearly observed. Thus, by choosing appropriate values of Δ we can select both regimes of growth. The existence of these two different regimes can be also confirmed by looking at the behavior of the tip velocity as a function of the undercooling or the Péclet number.

We have looked at the shape of the studied dendrites by computing the coordinates (X,Z), as defined above following Ref. [30]. Thus, only data of active branches are taken into account, i.e., branches longer than any other closer to the tip.

Figure 3 shows the plot of Z/R vs X/R for three different values of the undercooling $(\Delta=0.48,0.55,0.625)$. The representation for each Δ contains data from eight different times, which explains the slight dispersion of points. The existence of two regimes for each undercooling can be distinguished in Fig. 3, becoming more evident as the undercooling is increased. For small values of Z/R, similar behaviors are found

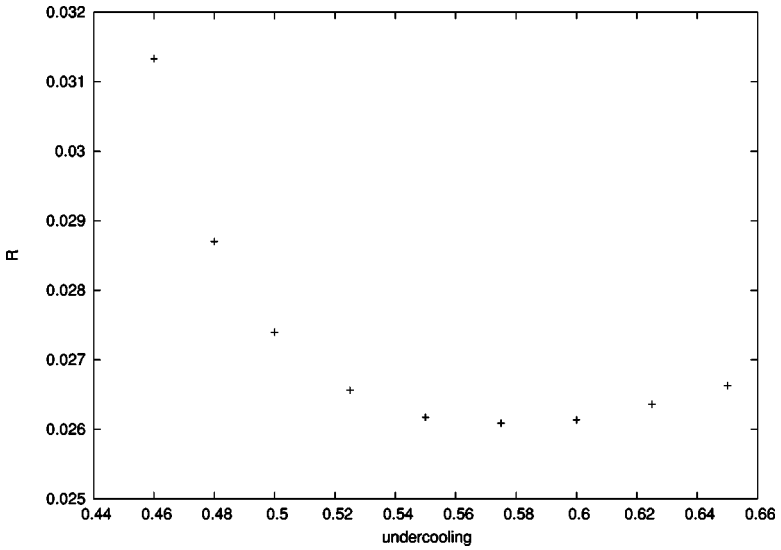

FIG. 2. Tip radius of the dendrite vs undercooling.

for all the undercoolings. However, from a certain value of Z/R, X/R depends very much on Δ. The transition region between both regimes is not clear enough to permit the precise location of a crossover point in this figure.

In order to better characterize the two observed regimes, Fig. 4 shows the log-log plot of X/R vs Z/R for the smallest and the largest undercoolings presented in Fig. 3.

It can be observed from Fig. 4 that a clear change in the behavior of X/R occurs in the regions of Z/R around 80 and 40 for the case of small and large undercoolings, respectively. This suggests that these regions separate two zones A and B (see Fig. 4) where sidebranching is in different regimes. For $\Delta \leqslant 0.48$ it is difficult to distinguish these two regimes because their slopes are very similar and it is not possible to determine a transition region. When the undercooling is increased it is found that the transition region is closer to the tip, which is consistent with the fact that at larger undercoolings a more developed sidebranching is obtained.

The behavior of X/R in region A is not exactly the same for all the considered undercoolings and is given by a straight line in the log-log plot. By comparing data from different undercoolings, it can be observed that the set of points in region A lies at larger values of X/R in the case of larger Δ. This is consistent with observations reported in Ref. [34,35], where the exponents a calculated for each single branch in $x \sim t^a$, x being the branch length and t being the time, were systematically smaller in branches grown in lower undercooling conditions. According to this, at any value of the undercooling and at small Z/R, points in the $X/R(Z/R)$ representation are less dispersed than at large Z/R because in the region closer to the tip it is still too soon to see the effects of the difference in the exponent a of each branch. Thus, the

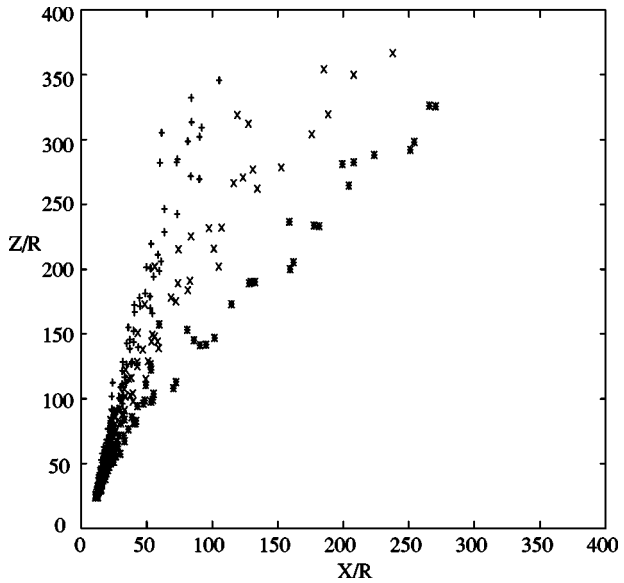

FIG. 3. Plot of Z/R vs X/R for the sidebranches that are larger than any others closer to the tip. Symbols $+$, $\times$, and $*$ correspond to $\Delta = 0.48$, 0.55, and 0.625, respectively.

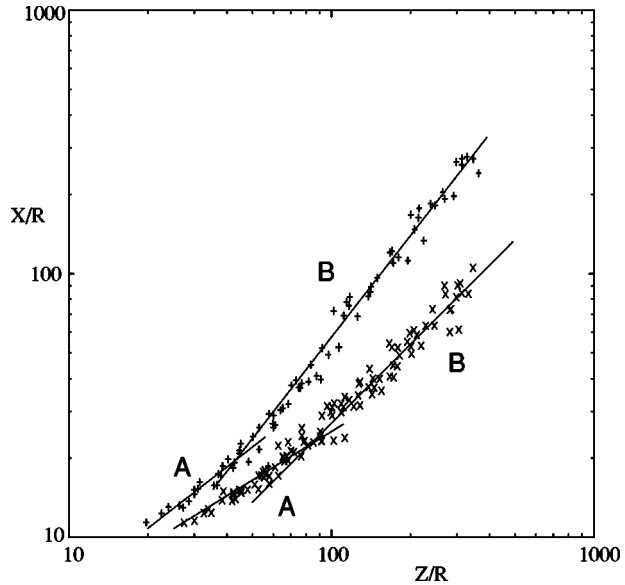

FIG. 4. Log-log plot of X/R vs Z/R for the sidebranches that are larger than any others closer to the tip. Symbols $\times$ and $+$ correspond to $\Delta = 0.48$ and 0.65, respectively. In each case, regions A and B are indicated.

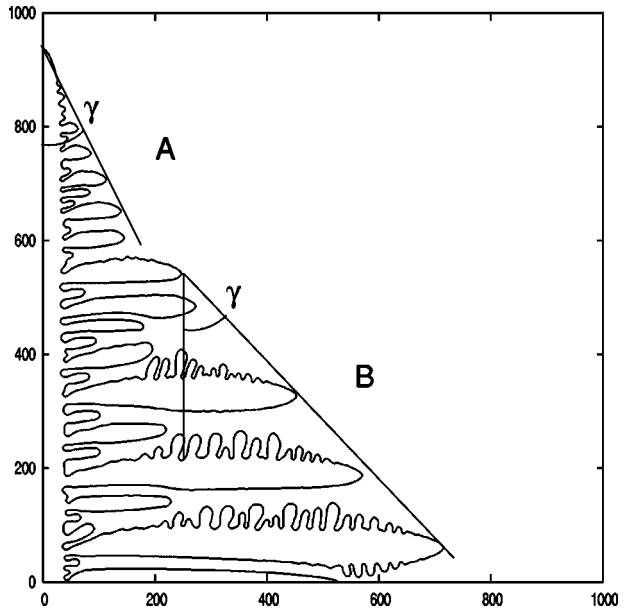

FIG. 5. Dendrite grown at $\Delta=0.6$ where regions A and B are indicated. Angle γ is always larger in regions B, where its value tends to 45° as the undercooling is increased.

dispersion of points must increase with Z/R, as can also be observed in Fig. 3.

The behavior of X/R in region B depends on Δ. When fitting the points of region B to $X/R \sim (Z/R)^{\alpha}$ we found that values of α tended to 1 for increasing Δ (in fact, from $\Delta \geqslant 0.525$, variations in α are very small). In Fig. 5 is shown a dendrite grown at $\Delta=0.6$ where regions A and B can be clearly distinguished. It can be observed that the angle γ formed by the line joining the tips of active sidebranches and the axis of the main arm is smaller in the region A and, typically for this range of undercoolings, its value is very close to 45° in the region B. In other words, in region B sidebranches grow at the same velocity that the main tip, i.e., grow as free dendrites.

The observation of these two regimes reveals a significant difference with experiments presented in Ref. [30] (see Fig. 7 there), where only one regime was observed, and the angle formed by the axis of the main arm and the line joining the tips of the branches was always considerably smaller than 45°. This has to be related to the small values of undercooling used in these experiments. The diffusion lengths associated with such a slow growth are very large, and even in the region furthest from the tip considered in the experiments the process of competition between branches was not finished yet. On the contrary, diffusion length in simulations is short due to the large undercoolings used. Branches can grow as free dendrites as long as distances between active sidebranches (which increase with the distance to the tip due to the competition process) are larger than the interaction scale given by the diffusion length (which is reduced for larger growth velocities). This results as the condition for the zone B to be observed.

We have also measured the integral parameters (contour length U and area F) of our two-dimensional dendrites. As shown in Fig. 1, U is the length of the contour of the dendrite

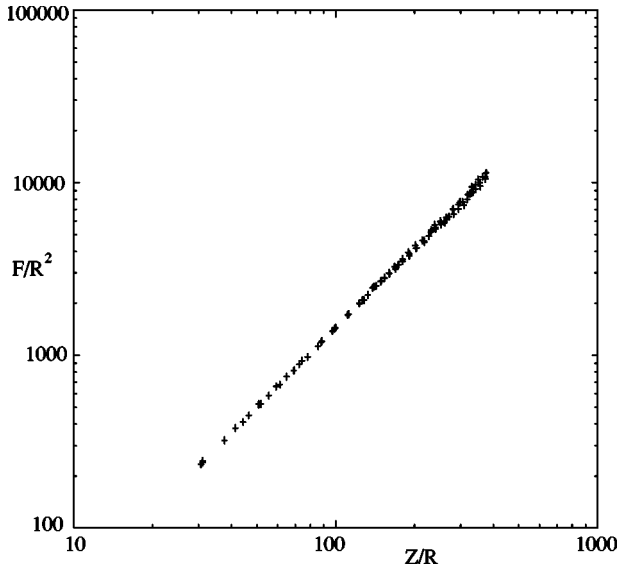

FIG. 6. Log-log plot of F/R^2 vs Z/R, F being the surface area, for $\Delta=0.525$.

measured from the tip to a distance Z along the axis, while F is one-half of the area of the dendrite. Both magnitudes have been measured for different values of the dimensionless undercooling. Considering the origin of coordinates at the tip, the contour length and the area have been calculated from the coordinates of the dendrite contour by

$$U = \sum_{i=1}^{n} [(Z_{i+1} - Z_i)^2 + (X_{i+1} - X_i)^2]^{1/2} \tag{3.1}$$

and

$$F = \sum_{i=1}^{n} \frac{(X_{i+1} + X_i)}{2}(Z_{i+1} - Z_i), \tag{3.2}$$

where n corresponds to each distance to the tip for which we calculated U and F. The fact that the shape of sidebranches is rather irregular and that their growth is not always perpendicular to the y axis makes it difficult to define U and F in a unique way everywhere as a function of Z. In order to better define both functions and following Ref. [30], we have only considered U and F for the values of Z corresponding to valleys between two neighboring sidebranches.

In Fig. 6 is shown the log-log plot of the normalized value of the surface area as a function of the normalized value of the distance to the tip of the dendrite at $\Delta=0.525$ with data taken at three different times. The same representation for the rest of the considered undercoolings shows the same behavior and only points far from the tip at larger Δ are slightly dispersed.

F/R^2 vs (Z/R) follows a power law $(a \sim b^c)$ where c is always around 1.5, although a slight tendency to increase with Δ is also observed. The value of c found in the simulations completely coincides with that found in Ref. [22] for the growth of ammonium bromide crystals in two dimensions. However, in Refs. [30,31] the representation of $F/R^2(Z/R)$ showed two regimes of power-law behavior with

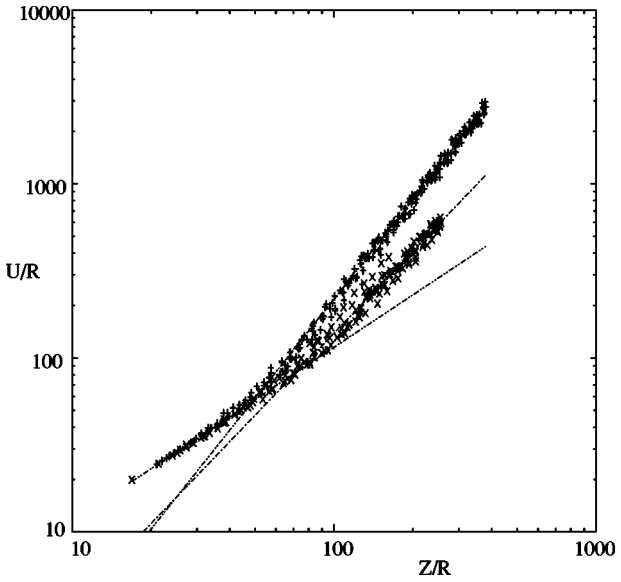

FIG. 7. Log-log plot of U/R vs Z/R, U being the contour length. Symbols $\times$ and $+$ correspond to $\Delta=0.44$ and 0.6, respectively. Lines indicate the fitting of points in each region.

different exponents. In principle, we should not expect to find the same exponent in our simulations, taking into consideration that these experiments were three dimensional and the projection area of the dendrite was measured. In this case, the existence of different regimes near and far from the tip of the dendrite was attributed to the different effect of coarsening. This effect is also present in two dimensions, but the fact that only one regime is observed in the plot of F/R^2 makes us conclude that the manifestation of the coarsening effect is less dramatic in two than in three dimensions. As regards the prefactor of the power-law fitting, it shows a similar behavior to that of the tip radius, that is, it decreases when the undercooling is increased up to $\Delta<0.55$ and it increases for larger Δ.

The behavior of the normalized contour length as a function of the distance to the tip for $\Delta=0.44$ and 0.6 is shown in Fig. 7. As happened in the plot of the shape of the dendrite, the behavior changes after a transition region, the variation of U/R being larger in the regions further down from the tip.

In the region closer to the tip, it is found that $U/R \sim (Z/R)^1$, which coincides with the behavior found in the linear regime of experiments in Ref. [31]. As one should expect, simulation results show that the linear region is larger for smaller undercoolings. This was not observed in Ref. [31], probably due to the employed range of undercoolings.

After the linear region, there is a transition region which is followed by a nonlinear region, as was observed in the experiments (see Fig. 5 in Ref. [31]). The transition region in the $U/R(Z/R)$ plot is at smaller values of Z/R than the transition region in the $X/R(Z/R)$ plot (Fig. 4) for all the considered undercoolings. In fact, the change in the behavior of the contour length and that of the shape of the dendrite (the envelope of it) provide different information of the sidebranching activity. In the case of U, the linear and nonlinear regimes are associated with low and high developed perturbations of the interface, respectively. In the nonlinear region, both active and nonactive branches contribute to the calculation of U. The enhanced growing of the active branches observed in the nonlinear region is accompanied by coarsening, a process in which the shrinking of the shorter branches reduces the total increasing of the contour length. As a result any nonlinearity has an effect on the behavior of U. On the contrary the shape $X/R(Z/R)$ is calculated through the active branches only. $X/R(Z/R)$ is then associated with the effect on the winning branches of competition, and with these larger branches reaching colder regions and hence growing faster. As a result, dispersions of X/R values are rather large, and the change of behavior more difficult to locate with a tendency to occur inside the nonlinear region. The behavior of U/R in the nonlinear region can be fitted by a power law (see Fig. 7), although the values of the prefactor and the exponent depend on the undercooling. As regards the prefactor, its variation with Δ is very similar to that of the tip radius, that is, it decreases up to $\Delta\sim0.55$ (surface tension dendrites) and it increases at larger undercoolings (kinetic dendrites). The largest value of the prefactor is 0.101 for $\Delta=0.44$, which is very far from the value obtained in Ref. [31]. The divergence is probably related to the different ranges of undercoolings used in simulations and experiments, but the difference in dimensions could also play a role.

As regards the exponent in the fitting of U/R, it increases with the undercooling from 1.57 to 1.89. The value for small Δ is very similar to the unique value (1.50) obtained in experiments [31]. Again, the fact of having found many exponents in the simulations and only one in the experiments could be associated with the different ranges of Δ used. It implies that the diffusion length considerably varies between simulations and experiments. The influence of the diffusion length on the competition process between branches that takes place in the nonlinear region determines the evolution of branches and consequently the behavior of the contour length.

By combining the results of the integral parameters in the linear regime, it is found that $F/(UR)\sim(Z/R)^{0.5}$, which coincides with the experiments [31]. The same exponent in the nonlinear regime varies from -0.07 to -0.39, differing very much from the experiments. Thus, the similarities between our results and the experimental ones in Ref. [31] remain mainly in the linear region and in opposition to previous studies [26,30], where F/UR was found to be constant in the nonlinear regime.

IV. CONCLUDING REMARKS

We have presented a numerical study of the shape and sidebranching in regions at different distances from the tip of a solidifying dendrite by means of a phase-field model with a nonconserved noise term. We have characterized the dendrite by using the integral parameters and we have focused on dendrites grown in both the surface tension and kinetic regimes.

The behavior of the shape of the dendrite has been found to depend on the undercooling in the considered range. The different diffusion lengths make the competition process between sidebranches differ and thus the final shape of the

dendrite is affected. The region where the competition process is taking place (A) and that where it is finished and sidebranches evolve like free dendrites (B) have been clearly distinguished in our simulation results. The behavior observed in B is in agreement with theoretical predictions [16]. On the other hand, the main divergence with the available experiments [30] is precisely the existence of two behaviors in the nonlinear region. This discrepancy may be explained by the different range of undercoolings considered in experiments and simulations. In our simulations undercooling (and hence tip velocity) is larger, so diffusion length is smaller and the transition between both zones is expected to occur closer to the tip, becoming observable. Note that additional increasings of undercooling would reduce further the size of zone A, which then could not be considered as a separate scaling region. The area of the dendrite presented a unique behavior for all the considered undercoolings. As one would expect, it coincides with that of two-dimensional dendrites [22], although there is a slight discrepancy with three-dimensional dendrites, especially in regions far from the tip. The behavior $F/R^2 \sim (Z/R)^{1.5}$ found in our simulations is the same as if the dendrites had a smooth parabolic shape. Thus, we can conclude that the area of two-dimensional dendrites is basically independent of the appearance and competition of sidebranches, and that situation does not depend on the diffusion length of the system.

The behavior of the contour length presents two differentiated regimes in the linear and nonlinear regions. The exponents found in the linear region are in agreement with experiments [31], while the discrepancies appearing in the nonlinear region could come from the range of undercoolings or the dimensionality.

We have found that the behavior of the contour length changes in regions closer to the tip than the behavior of the shape does. The picture is the following. As one moves down from the tip, one first finds the linear region where branches are created and eventually start to compete with each other. Going further, the nonlinear region appears after a transition region. The competition process is not only still taking place there but it is probably in the highest point of activity. Not so far away, its effects will be easily seen by the observation of some already stopped sidebranches. During all this way we have moved from the linear to the nonlinear region, but we are still in the region we called A. Further down, the competition process between branches is finished and the surviving ones have no opposition in their neighborhood to keep growing as free dendrites. We are then in region B.

Finally, we have considered both surface tension and kinetic dominated dendrites. Although the different behaviors of the studied parameters are observed when the undercooling is changed, this cannot be associated with the type of dendrite. All we can assure is that the linear and A regions in surface tension dendrites will always be larger than in the kinetic ones, but only because of the larger diffusion length and not because of the main mechanism which determines them.

These results offer some insight into the understanding of a fully developed dendrite, and in particular are of relevant importance to distinguish between low and high undercooling dendrites and two-dimensional and three-dimensional dendrites. Finally we should remark that it would be of the most great interest to have more experimental results available in the high undercooling regime, in particular characterizing the nonlinear regions of the dendrite.

ACKNOWLEDGMENTS

The authors acknowledge discussions with Y. Couder. This research was supported by the Dirección General de Investigación Científica y Técnica (Spain) (Project No. BFM2003-07850-C03-02) and Comissionat per a Universitats i Recerca (Spain) (Project No. 2001SGR00221).

[1] J.S. Langer, in *Chance and Matter*, 1986 Les Houches Lectures, edited by J. Souletie, J. Vannimenus, and R. Storra, (North-Holland, Amsterdam, 1987), Chap. 10, pp. 629–711.
[2] *Dynamics of Curved Fronts*, edited by P. Pelcé, Perspectives in Physics (Academic, New York, 1988).
[3] E. Ben-Jacob and P. Garik, Nature (London) **343**, 523 (1990).
[4] E.A. Brener and V.I. Melnikov, Adv. Phys. **40**, 53 (1991).
[5] *Solids far from Equilibrium*, edited by C. Godrèche (Cambridge University Press, Cambridge, U.K., 1992).
[6] *Handbook of Crystal Growth*, edited by D.T.J. Hurle (North-Holland, Amsterdam, 1993).
[7] *Spatio Temporal Patterns*, edited by P.E. Cladis and P. Palffy-Muhoray, Santa Fe Institute Studies in the Science of Complexity Vol. 21 (Addison-Wesley, Reading, MA, 1994).
[8] J.S. Langer and H. Müller-Krumbhaar, Phys. Rev. A **27**, 499 (1983).
[9] W.J. Boettinger, S.R. Coriell, A.L. Greer, A. Karma, W. Kurz, M. Rappaz, and R. Trivedi, Acta Mater. **48**, 43 (2000).
[10] R. Pieters and J.S. Langer, Phys. Rev. Lett. **56**, 1948 (1986).
[11] O. Martin and N. Goldenfeld, Phys. Rev. A **35**, 1382 (1987).
[12] M.N. Barber, A. Barbieri, and J.S. Langer, Phys. Rev. A **36**, 3340 (1987).
[13] J.S. Langer, Phys. Rev. A **36**, 3350 (1987).
[14] R. Pieters, Phys. Rev. A **37**, 3126 (1988).
[15] W. van Saarloos, B. Caroli, and C. Caroli, J. Phys. I **3**, 741 (1993).
[16] E. Brener and D. Temkin, Phys. Rev. E **51**, 351 (1995).
[17] A. Karma and W.-J. Rappel, Phys. Rev. E **60**, 3614 (1999).
[18] S.G. Pavlik and R.F. Sekerka, Physica A **268**, 283 (1999).
[19] S.G. Pavlik and R.F. Sekerka, Physica A **277**, 415 (2000).
[20] R. González-Cinca, L. Ramírez-Piscina, J. Casademunt, and A. Hernández-Machado, Phys. Rev. E **63**, 051602 (2001).
[21] A. Dougherty, P.D. Kaplan, and J.P. Gollub, Phys. Rev. Lett. **58**, 1652 (1987).
[22] Y. Couder, F. Argoul, A. Arnéodo, J. Maurer, and M. Rabaud, Phys. Rev. A **42**, 3499 (1990).
[23] X.W. Qian and H.Z. Cummins, Phys. Rev. Lett. **64**, 3038 (1990).

[24] Ph. Bouissou, A. Chiffaudel, B. Perrin, and P. Tabeling, Europhys. Lett. **13**, 89 (1990).
[25] A. Dougherty and R. Chen, Phys. Rev. A **46**, R4508 (1992).
[26] E. Hürlimann, R. Trittibach, U. Bisang, and J.H. Bilgram, Phys. Rev. A **46**, 6579 (1992).
[27] L.M. Williams, M. Muschol, X. Qian, W. Losert, and H.Z. Cummins, Phys. Rev. E **48**, 489 (1993).
[28] U. Bisang and J.H. Bilgram, Phys. Rev. Lett. **75**, 3898 (1995).
[29] U. Bisang and J.H. Bilgram, Phys. Rev. E **54**, 5309 (1996).
[30] Q. Li and C. Beckermann, Phys. Rev. E **57**, 3176 (1998).
[31] Q. Li and C. Beckermann, Acta Mater. **47**, 2345 (1999).
[32] J.C. LaCombe, M.B. Koss, J.E. Frei, C. Giummarra, A.O. Lupulescu, and M.E. Glicksman, Phys. Rev. E **65**, 031604 (2002).
[33] R. González-Cinca and Y. Couder, in *Interface and Transport Dynamics: Computational Modelling*, edited by H. Emmerich, B. Nestler, and M. Schreckenberg, Lecture Notes in Computational Science and Engineering Vol. 32 (Springer-Verlag, Berlin, 2002), pp. 20–25.
[34] Y. Couder, J. Maurer, R. González-Cinca, and A. Hernández-Machado (unpublished).
[35] R. González-Cinca, A. Hernández-Machado, and Y. Couder (unpublished).
[36] R. González-Cinca, in *Emergent Nature*, edited by M.M. Novak (World Scientific, Singapore, 2002), pp. 357–364.
[37] R. González-Cinca, Physica A **314**, 284 (2002).
[38] R. Kobayashi, Physica D **63**, 410 (1993).
[39] A.A. Wheeler, B.T. Murray, and R.J. Schaefer, Physica D **66**, 243 (1993).
[40] A. Karma and W.J. Rappel, Phys. Rev. E **53**, R3017 (1996).
[41] T. Tóth-Katona, T. Börzsönyi, Á. Buka, R. González-Cinca, L. Ramírez-Piscina, J. Casademunt, A. Hernández-Machado, and L. Kramer, Phys. Rep. **337**, 37 (2000).
[42] R. González-Cinca, Ph.D. Thesis, Department of Applied Physics, Technical University of Catalonia, 2000 (unpublished).
[43] A. Karma, Phys. Rev. Lett. **87**, 115701 (2001).
[44] R. González-Cinca, R. Folch, R. Benítez, L. Ramírez-Piscina, J. Casademunt, and A. Hernández-Machado, in *Advances in Condensed Matter and Statistical Mechanics*, edited by E. Korucheva and R. Cuerno (Nova Science Publishers, New York, 2004), pp. 203–236, cond-mat/0305058.
[45] R. González-Cinca and L. Ramírez-Piscina (unpublished).
[46] W.H. Press, S.A. Teukolsky, W.T. Vetterling, and B.P. Flannery, *Numerical Recipes in Fortran* (Cambridge University Press, Cambridge, U.K., 1992).